

Coupled controls of climate, geology, and biota on late Pleistocene alluvial fan morphodynamics along the coast of the hyperarid Atacama Desert



***Janek Walk¹, Melanie Bartz², Georg Stauch¹, Mark Reyers³, Steven A. Binnie⁴,
Dominik Brill², Paulina Vásquez⁵, Fernando A. Sepúlveda⁵, Dirk Hoffmeister²,
Helmut Brückner², Frank Lehmkühl¹***

¹Department of Geography, RWTH Aachen University, Germany

²Institute of Geography, University of Cologne, Germany

³Institute of Geophysics and Meteorology, University of Cologne, Germany

⁴Institute of Geology and Mineralogy, University of Cologne, Germany

⁵Servicio Nacional de Geología y Minería, Santiago, Chile, Germany

Explanations: Click on for audio comments (requires Adobe Flash Player®)

© Authors.
All rights reserved.

Coastal alluvial fans (CAF) as geo-archives



Allogenic (environmental) controls

Biota

Geology

Climate

Characteristics

- CAF surface morphology
- CAF stratigraphy
- Catchment hydro-morphometry
- Spatial trends

Archive functions

- Magnitude, frequency, and types of primary processes
- Secondary processes
- Timing of fan development
- Coastal tectonic uplift

Autogenic (intrinsic) controls

G

(Walk et al., 2020)



F



E



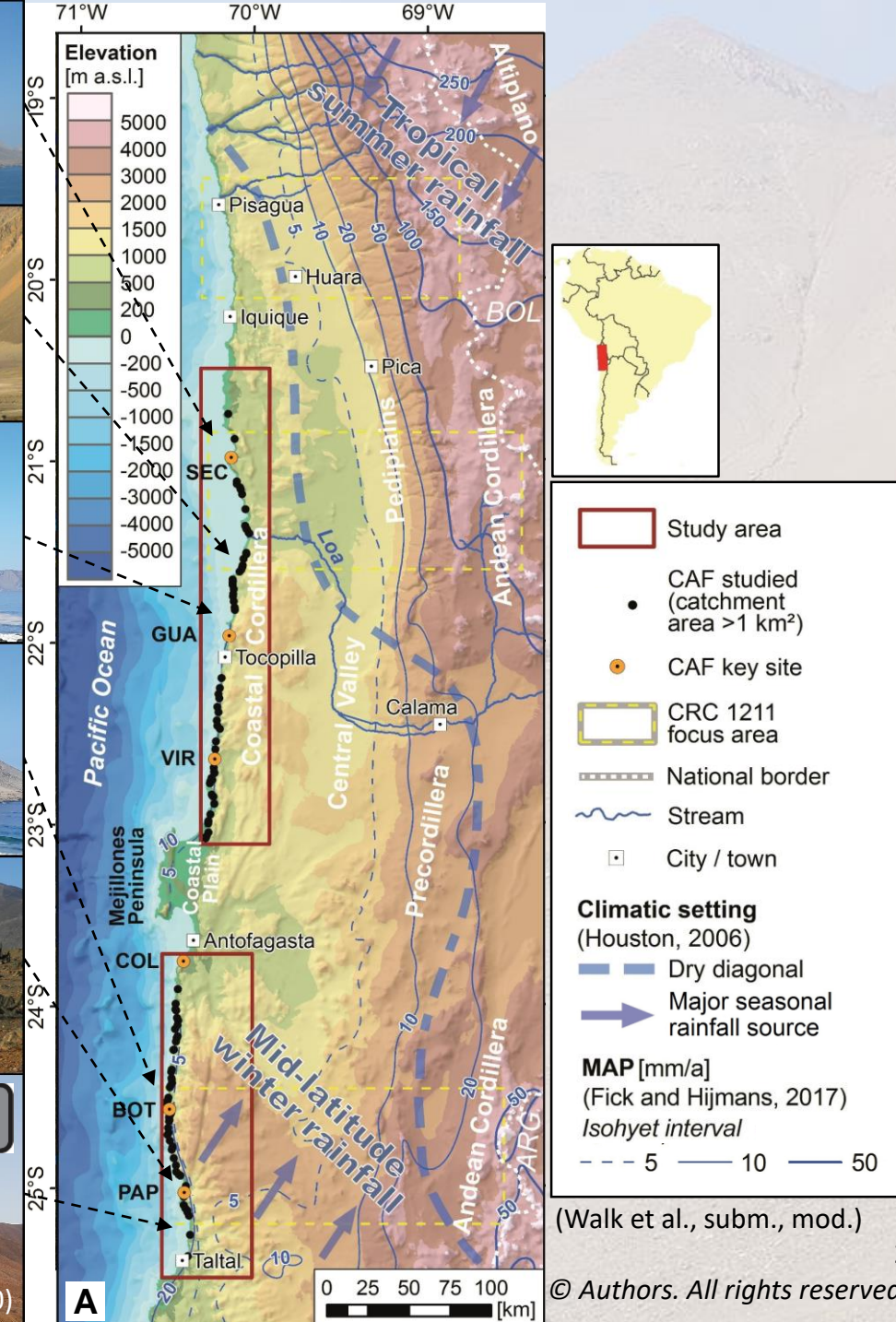
D



C



B

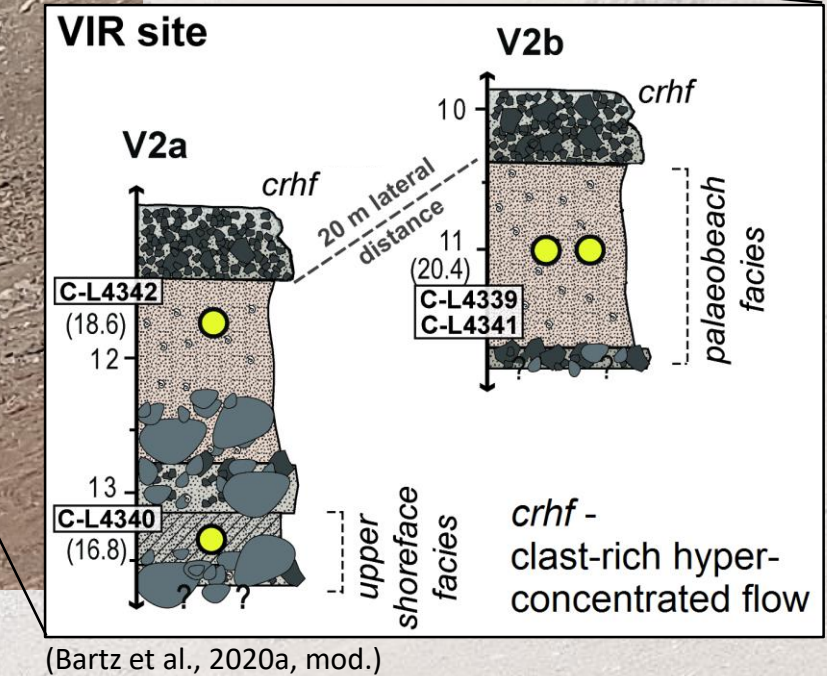


(Walk et al., subm., mod.)

2

© Authors. All rights reserved.

CAF as geo-archives in the hyperarid Atacama Desert – Caleta El Fierro (VIR)



Material and methods

TanDEM-X World DEM™
(DLR, 2017)

Regional Weather Research
and Forecasting (WRF)
climate model (Reyers, 2019)

Regional geological maps
(diverse sources, cf. slide 7)

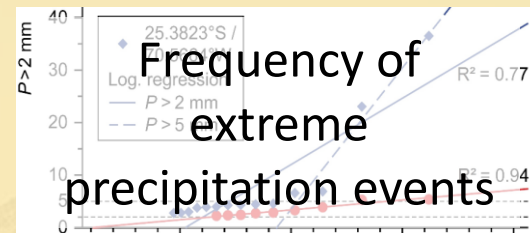
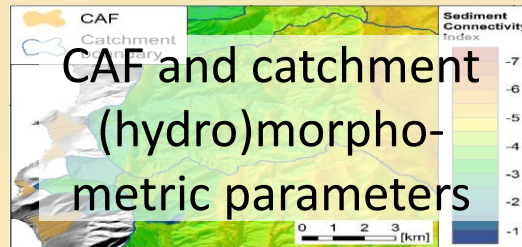
(Uplift rates derived from
dated marine terraces)
(Regard et al. 2010; Bartz et al., 2020a)

(Geobotanic studies on
Loma vegetation)
(Schulz et al., 2011)



Gradient analysis

(Walk et al., 2020)



Source-area
lithology and fault
density

(Regional tectonic
uplift)

(Vegetation density)



Geochronology

^{10}Be surface exposure
dating

(Bartz et al., 2020a; Walk et al., in prep.)

^{14}C dating

(Vargas et al., 2006; Vásquez et al., 2018;
Walk et al., in prep.)

Luminescence (pIR-IRSL)
(and quartz ESR) dating

(Bartz et al., 2020a, b; Walk et al., in prep.)

CAF and catchment (hydro)morphometric parameters

CAF morphometry

a_f – Area
 $VRM_f(3)$ – Mean vector ruggedness measure (3 x 3 kernel)
 g_f – Mean gradient
 R_f – Relief

For details on parameters see Walk et al. (2020)

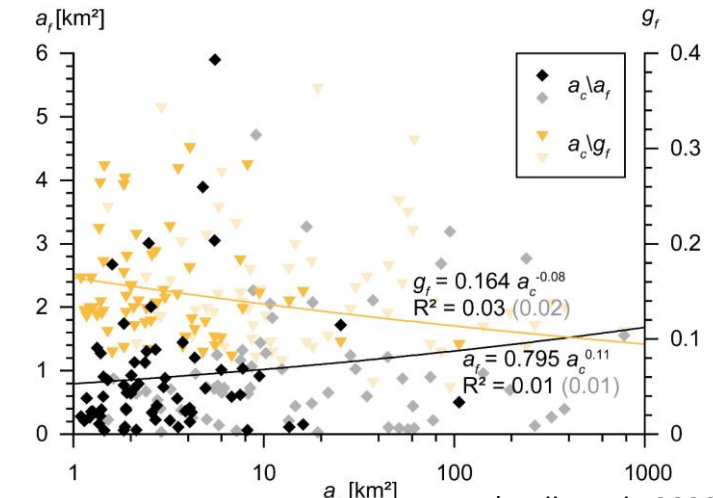


Catchment hydromorphometry

a_c – Area
 g_c – Gradient
 $h_{c,min}$ – Minimum elevation
 HI_c – Hypsometric index
 rr_c – Basin relief ratio
 $StdCTI_c$ – Mean standardized compound topographic index
 $VRM_c(5)$ – Mean vector ruggedness measure (5 x 5 kernel)
 Cl_c – Circularity index
 $IC_{c,Dinf}$ – Mean index of sediment connectivity
 kzd_{25} – Knickzone density (d interval = 25 m)
 dd – Drainage density

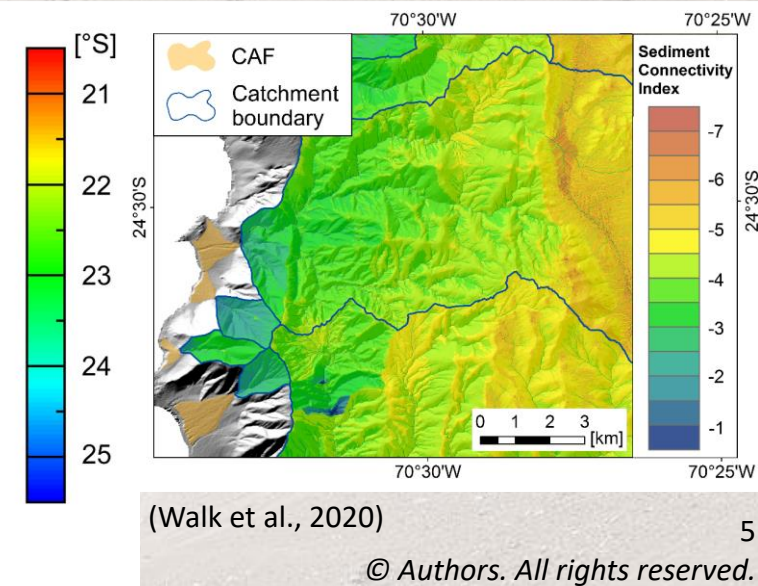
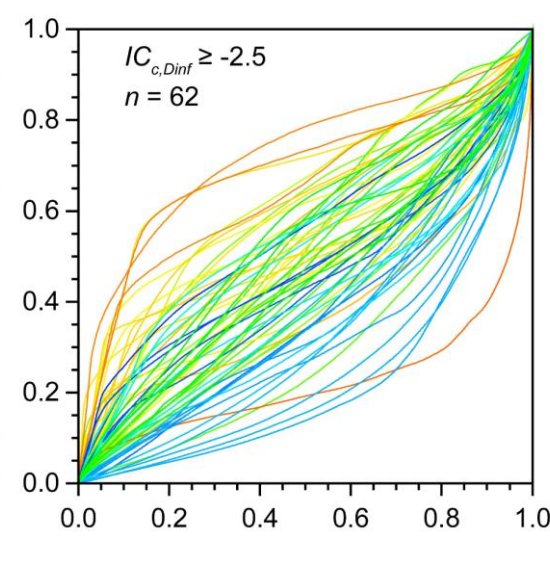
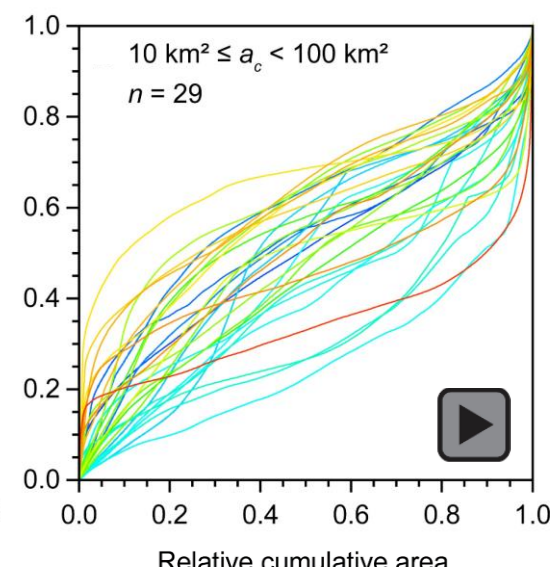
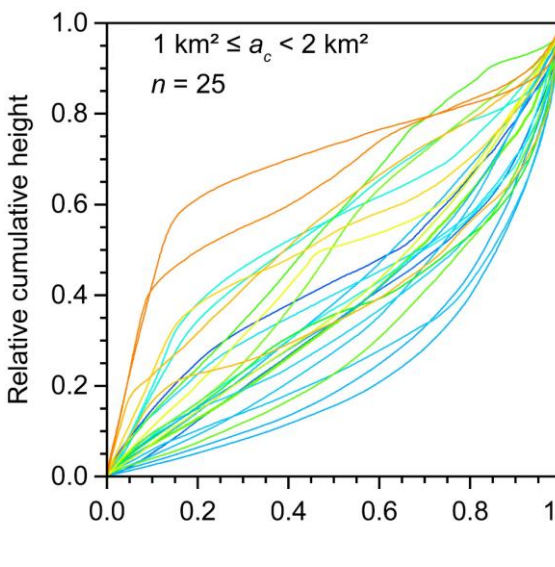


CAF-catchment relationships



(Walk et al., 2020)

Catchment hypsometry



(Walk et al., 2020)

© Authors. All rights reserved.

Climatic control: Frequency of extreme precipitation events

Climatic parameters

- Based on frequency analysis of 36 a WRF precipitation time series (Reyers, 2019)
 - Temporal resolution: daily
 - Spatial resolution: 10 km

P – Precipitation (event)

RI – Recurrence interval

P^* – Expected precipitation

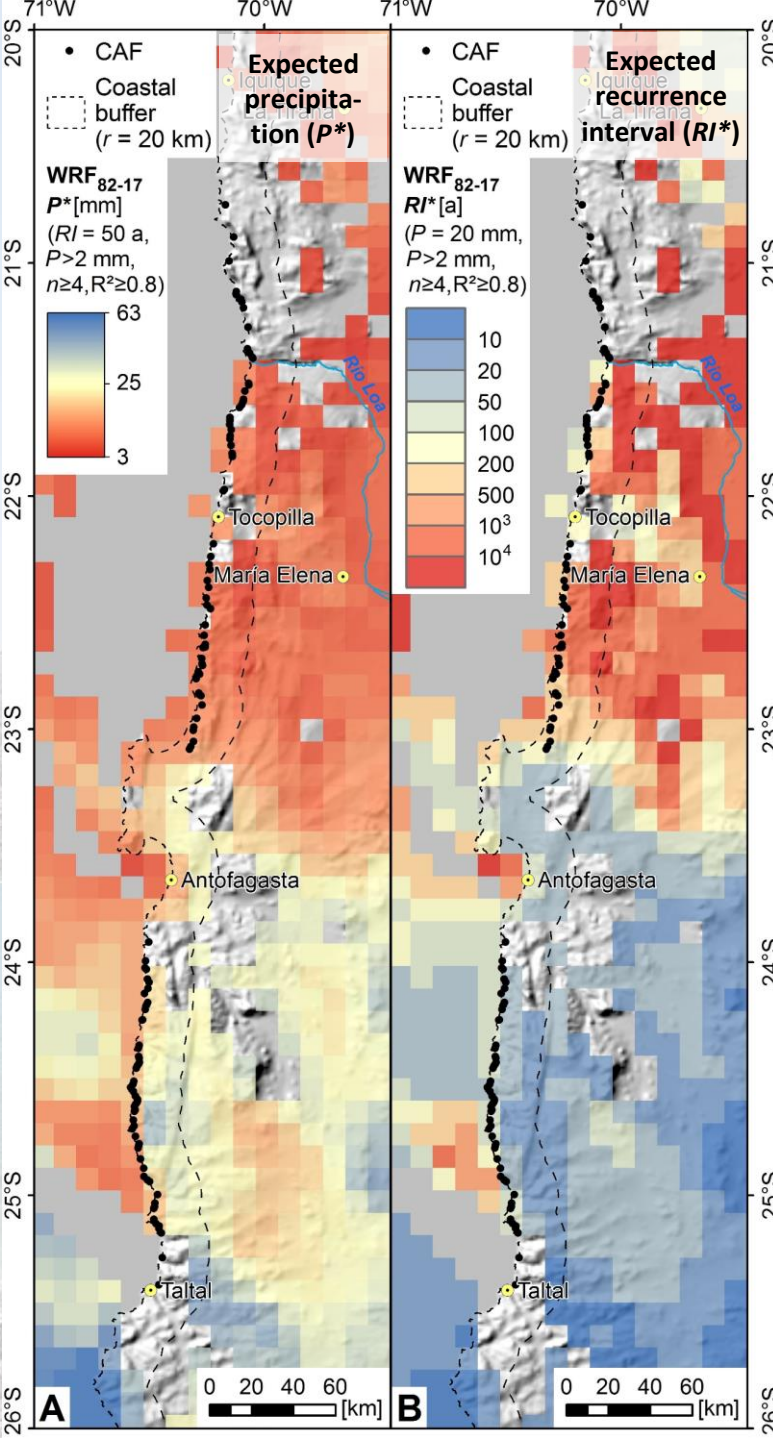
RI^* – Expected recurrence interval

MAP – Mean annual precipitation

$n_{>20mm}$ – Number of events with $P > 20 \text{ mm}$ (in WRF time series)

- For statistical analysis:

$p_{30a,10mm}^+$ – Distribution-free occurrence probability of an event with $P > 10 \text{ mm}$ in 30 a



(Walk et al., 2020)

© Authors. All rights reserved.

Geologic control: Source-area lithology and fault density

Geologic parameters

- Based on compilation of 13 regional geological maps (1:100k, 1:250k)
- Reclassification of catchment bedrock lithology (proportions)

g(1_) – Unconsolidated sediments

g(2+3) – Sedimentary rocks

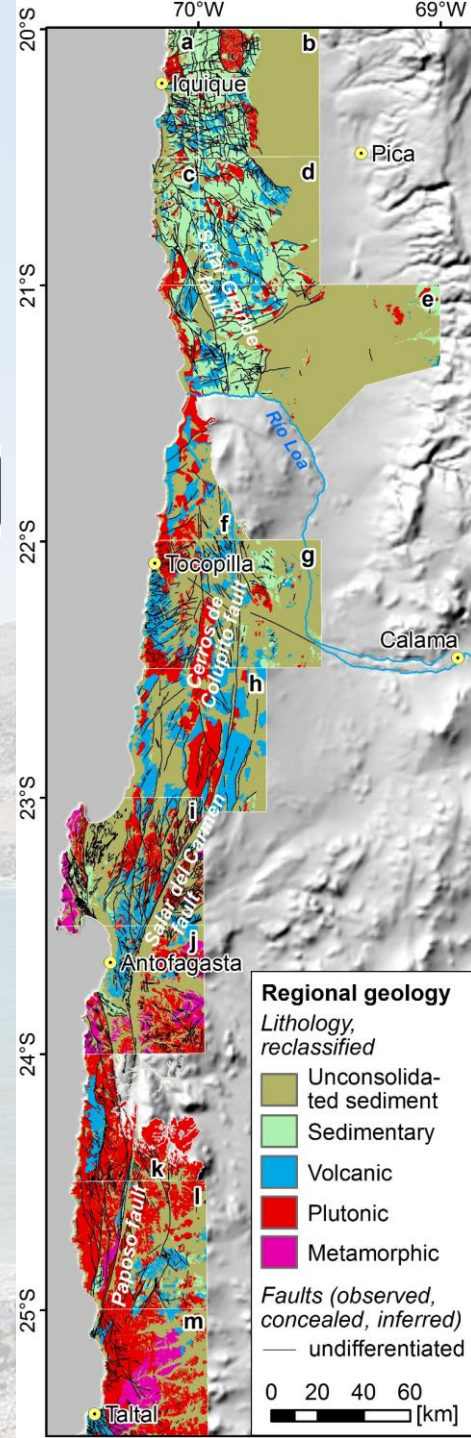
g(4_) – Volcanic rocks

g(5) – Plutonic rocks

g(6) – Metamorphic rocks

- Degree of faulting in catchments

fd – fault density

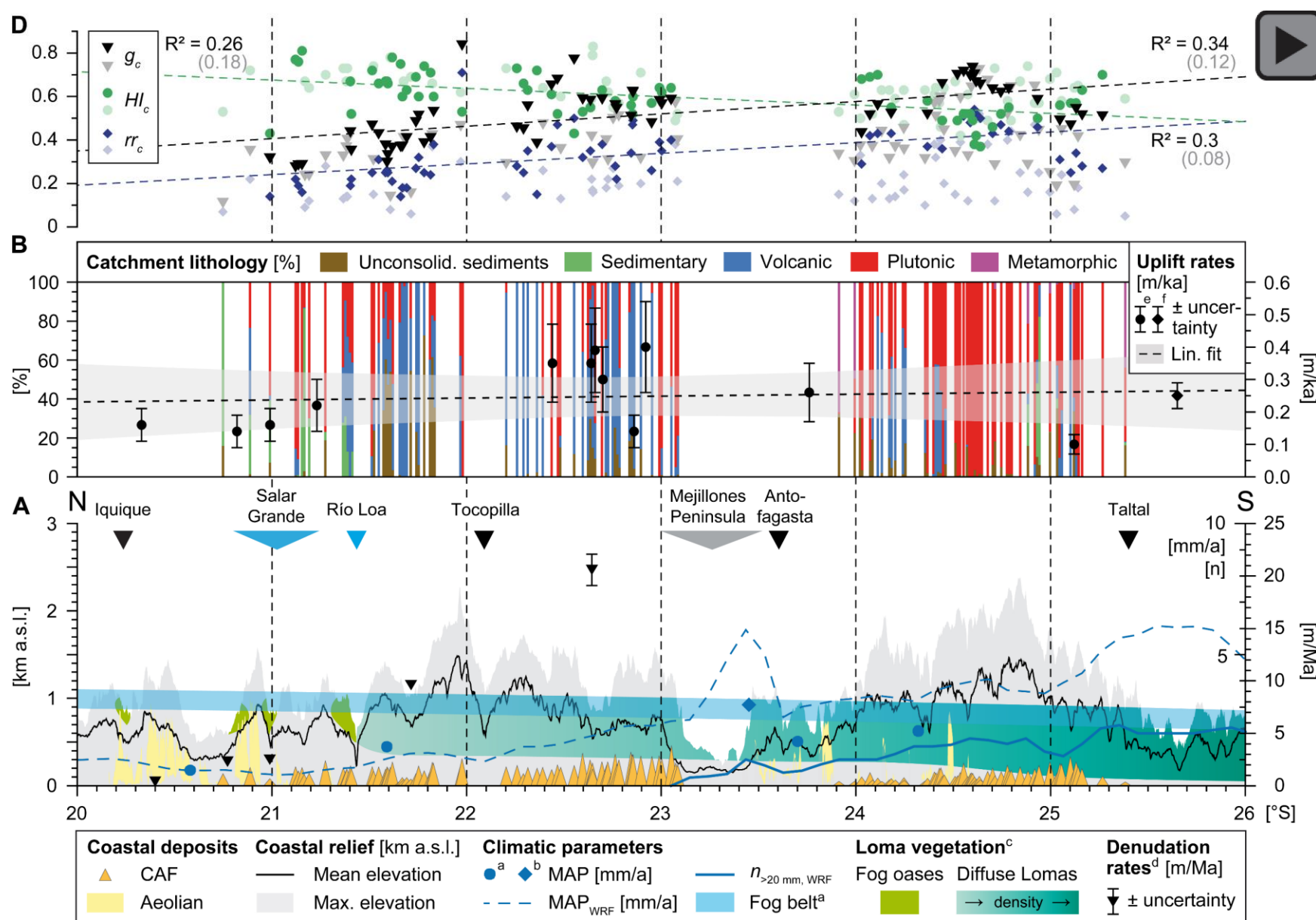


References

- a – Sepúlveda and Vásquez (2012)
- b – Vásquez and Sepúlveda (2012a)
- c – Vásquez and Sepúlveda (2012b)
- d – Sepúlveda et al. (2012)
- e – Quezada et al. (2012)
- f – Skarmeta and Marinovic (1981)
- g – Medina et al. (2012)
- h – Mpodozis et al. (2015)
- i – Cortés et al. (2007)
- j – González and Niemeyer (2005)
- k – Domagala et al. (2016)
- l – Álvarez et al. (2016)
- m – Escribano et al. (2013)

(Walk et al., 2020)

Results: Controls on CAF morphodynamics – Spatial gradient analysis



Results: Controls on CAF morphodynamics – Factor analysis

$ C_{c,Dinf} \geq -2.5$	$n = 62$	Factor 1	Factor 2	Factor 3	Factor 4	Factor 5
	Explained variance	0.24	0.16	0.10	0.07	0.06
CAF morphometric parameter	$\log a_f$	0.16	0.98	0.08	-0.03	0.07
	$VRM_f(3)$	0.02	-0.52	0.02	0.01	0.04
Catchment morphometric and hydrographic parameter	g_f	-0.05	-0.77	0.22	0.02	-0.06
	$\log R_f$	0.07	0.72	0.31	0.06	-0.02
Catchment geology	$\log a_c$	-0.50	0.14	-0.01	0.12	0.29
	g_c	0.95	0.12	-0.05	0.01	-0.01
WRF ₈₂₋₁₇	$\log h_{c,min}$	0.09	0.68	0.31	0.10	-0.01
	HI_c	-0.67	-0.05	-0.06	0.22	-0.03
	rr_c	0.95	-0.08	0.00	-0.04	-0.04
	$StdCTI_c$	-0.47	-0.35	-0.04	-0.13	0.08
	$VRM_c(5)$	-0.24	0.18	0.18	0.02	-0.06
	CI_c	0.59	0.05	-0.16	0.02	0.19
	kzd_{25}	0.83	0.20	0.00	-0.05	-0.06
	dd	-0.64	-0.16	0.22	-0.14	-0.12
	fd	0.02	0.02	-0.13	0.29	0.12
	$g(1)^*$	-0.14	0.12	0.83	-0.53	-0.07
	$g(2+3)^*$	0.05	-0.04	0.02	0.00	1.00
	$g(4)^*$	-0.09	0.05	0.20	0.95	-0.19
	$g(5)^*$	0.18	-0.14	-0.96	-0.15	-0.07
	$p_{30a,10mm}^+$	0.60	0.00	-0.19	0.24	0.03

* – centred log-ratio transformation applied prior to analysis

Bold type – factor loading value ≥ 0.59 or ≤ -0.59

(= components of factor)

(Walk et al., 2020)

CAF hydro-morphometry & frequency of extreme P

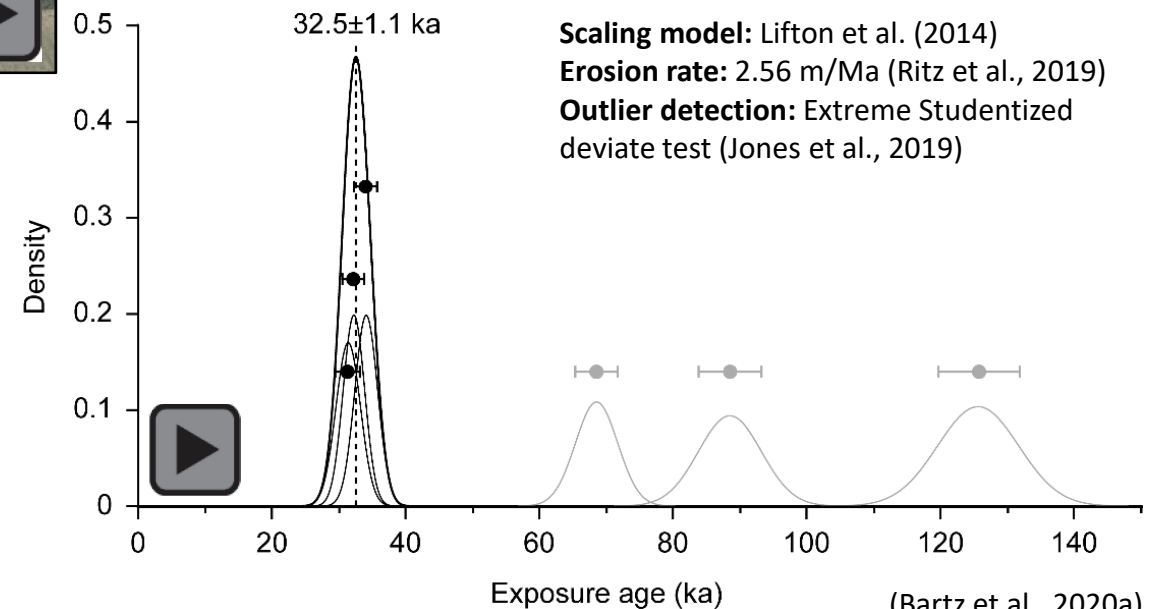
Interrelated CAF morphometry

Source-area lithology

Results: Geochronology – ^{10}Be surface exposure dating (BOT – Botija)



BOT CAF mean surface exposure age



(Bartz et al., 2020a)

Results: Geochronology – Luminescence dating (VIR – Caleta El Fierro)

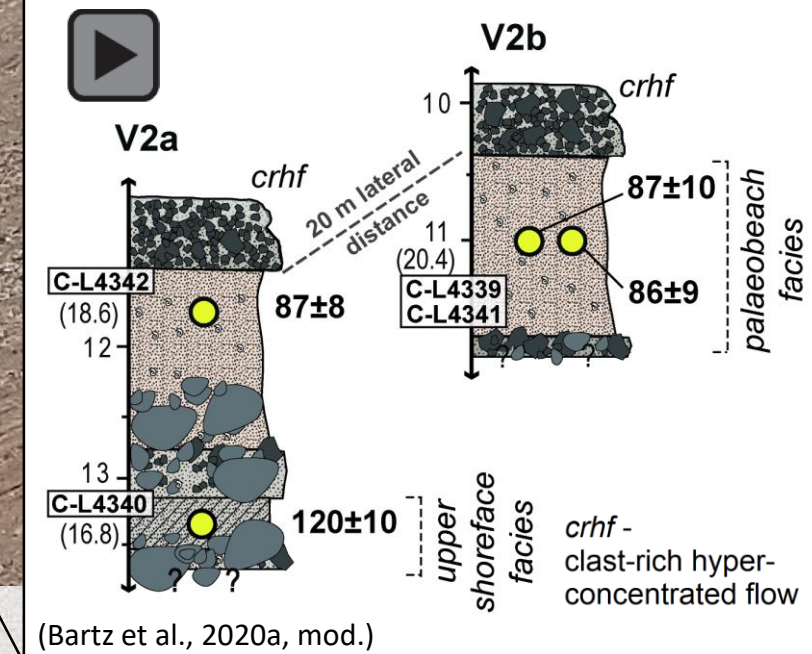


VIR site

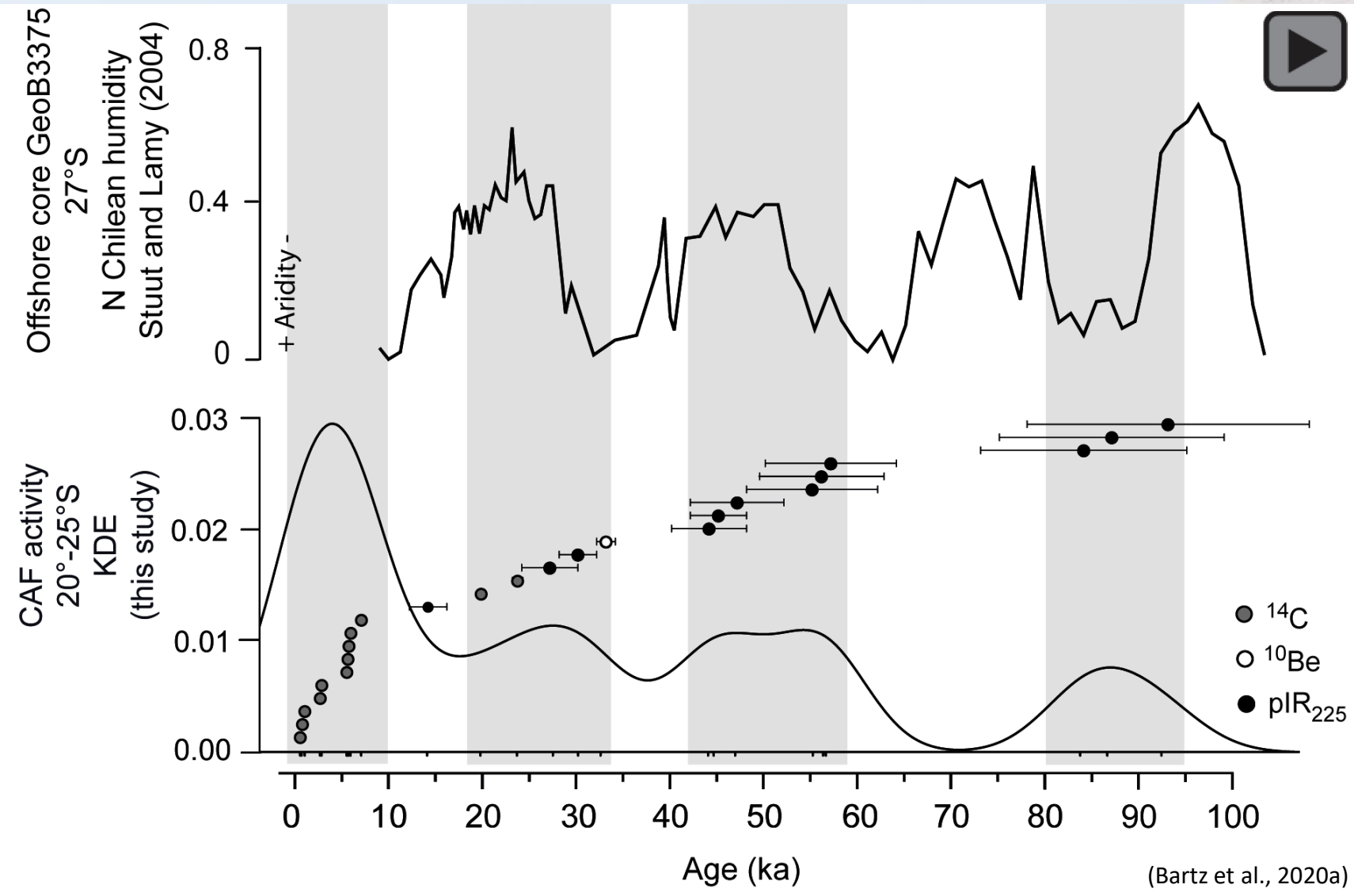
Protocol: pIR-IRSL₂₂₅ (Thomsen et al., 2008)

Fading correction: Huntley and Lamothe (2001),
Auclair et al. (2003)

Central age model: Galbraith et al. (1999)



Results: Geochronology – Synthesis and palaeoenvironmental interpretation



Conclusions

Allogenic controls

Climate

- Frequency of strong *P* events: **dominant**

Geology

- Source-area lithology: **negligible**
- Tectonics: **indirect**

Biota

- Positive feedback mechanisms: **indicated** (future work)

Autogenic controls

- Significance for specific CAF systems as yet unknown
- Future studies to discriminate case-specific from systematic regional geomorphic responses

Geo-archive functions – CAF of the Atacama Desert

- Magnitude, frequency, and types of primary processes
- Secondary processes
- Timing of fan development
- Coastal tectonic uplift





Acknowledgements

The project is part of the CRC 1211 ‘Earth – Evolution at the Dry Limit’ funded by the DFG (Grant-No.: 268236062–SFB 1211). The TanDEM-X WorldDEM™ data is provided by a DLR Science grant, 2017. E. Campos is thanked for helping to organize the field campaigns. J.-P. Francois as well as M. Keiser are gratefully acknowledged for assisting in field work. We further thank C. Mpodozis for providing a regional geological map for the area between 22.5 and 23°S.

References

- Álvarez, J. et al., 2016. Cartas Punta Posallaves y Sierra Vicuña Mackenna, Región de Antofagasta, Serie Geología Básica 183-184. Servicio Nacional de Geología y Minería, Santiago, pp. 147, 1 mapa escala 1:100.000.
- Auclair, M. et al., 2003. Measurement of anomalous fading for feldspar IRSL using SAR. *Radiat. Meas.* 37, 487–492.
- Bartz, M. et al., 2020a. Late Pleistocene alluvial fan evolution along the coastal Atacama Desert (N Chile). *Global Planet. Change*, in press.
- Bartz, M. et al., 2020b. Testing the potential of K-feldspar pIR-IRSL and quartz ESR for dating coastal alluvial fan complexes in arid environments. *Quatern. Int.*, in press.
- Cortés, J. et al., 2007. Cartas Mejillones y Península de Mejillones, Región de Antofagasta, Serie Geología Básica 103-104. Servicio Nacional de Geología y Minería, Santiago, pp. 58, 1 mapa escala 1:100.000.
- Deutsches Zentrum für Luft- und Raumfahrt (DLR), 2017. TanDEM-X Science Service System. URL: <https://tandemx-science.dlr.de/>.
- Domagala, J. et al., 2016. Cartas Blanco Encalada y Pampa Remiendos, Región de Antofagasta, Serie Geología Básica. Servicio Nacional de Geología y Minería, Santiago, pp. 187–188, 1 mapa escala 1:100.000.
- Escribano, J. et al., 2013. Cartas Bahía Isla Blanca y Taltal, Región de Antofagasta, Serie Geología Básica 164-165. Servicio Nacional de Geología y Minería, Santiago, pp. 75, 1 mapa escala 1:100.000.
- Fick, S.E., Hijmans, R.J., 2017. WorldClim 2: New 1-km spatial resolution climate surfaces for global land areas. *Int. J. Climatol.* 37., 4302–4315.
- Galbraith, R.F. et al., 1999. Optical dating of single and multiple grains of quartz from Jinmium rock shelter, northern Australia: Part I, experimental design and statistical models. *Archaeometry* 41, 339–364.
- Garreaud, R.D. et al., 2008. Interannual variability of the coastal fog at Fray Jorge relict forests in semiarid Chile. *J. Geophys. Res. Biogeosci.* 113, G04011.
- González, G., Niemeyer, H., 2005. Cartas Antofagasta y Punta Tetas, Región de Antofagasta, Serie Geología Básica 89. Servicio Nacional de Geología y Minería, Santiago, pp. 35, 1 mapa escala 1:100.000.
- Huntley, D.J., Lamothe, M., 2001. Ubiquity of anomalous fading in K-feldspars and the measurement and correction for it in optical dating. *Can. J. Earth Sci.* 38, 1093–1106.
- Houston, J., 2006. Variability of precipitation in the Atacama Desert: its causes and hydrological impact. *Int. J. Climatol.* 26, 2181–2198.
- Jones, R.S. et al., 2019. iceTEA: Tools for plotting and analysing cosmogenic-nuclide surface-exposure data from former ice margins. *Quat. Geochronol.* 51, 72–86.
- Lifton, N. et al., 2014. Scaling in situ cosmogenic nuclide production rates using analytical approximations to atmospheric cosmic-ray fluxes. *Earth Plan. Sci. Lett.* 386, 149–160.
- Medina, E. et al., 2012. Cartas Tocopilla y María Elena, Región de Antofagasta, Serie Geología Básica 141-142. Servicio Nacional de Geología y Minería, Santiago, pp. 59, 1 mapa escala 1:100.000.
- Mpodozis, C.M. et al., 2015. Mapa Geológico de la Cordillera de la Costa entre Tocopilla y Antofagasta, escala 1:250.000. Antofagasta Minerals, unpublished internal report.
- Quezada, A. et al., 2012. Mapa compilación geológica área Quillagua - Salar Grande, Región de Tarapacá. In: Blanco, N., et al. (Eds.), Levantamiento Geológico Para El Fomento de La Exploración de Recursos Minerales e Hídricos de La Cordillera de La Costa, Depresión Central y Precordillera de La Región de Tarapacá (20°S-21°S), Informe Registrado IR-12-50. Servicio Nacional de Geología y Minería, Santiago, pp. 246, 7 mapas escala 1:100.000.
- Regard, V. et al., 2010. Renewed uplift of the Central Andes Forearc revealed by coastal evolution during the Quaternary. *Earth Planet. Sci. Lett.* 297, 199–210.

References

- Reyers, M., 2019. WRF Output daily accumulated total precipitation 10km Atacama. CRC1211 Database (CRC1211DB). <https://doi.org/10.5880/CRC1211DB.20>.
- Ritz, J.-F. et al., 2019. Slip rate of trench-parallel normal faulting along the Mejillones Fault (Atacama Fault System): Relationships with the northern Chile subduction and implications for seismic hazards. *Terra Nova* 31, 390–404.
- Schulz, N. et al., 2011. Phytogeographic divisions, climate change and plant dieback along the coastal desert of northern Chile. *Erdkunde* 65, 169–187.
- Sepúlveda, F.A., Vásquez, P., 2012. Mapa geológico de Iquique, Región de Tarapacá. In: Blanco, N., et al. (Eds.), *Levantamiento Geológico Para El Fomento de La Exploración de Recursos Minerales e Hídricos de La Cordillera de La Costa, Depresión Central y Precordillera de La Región de Tarapacá (20°S-21°S)*, Informe Registrado IR-12-50. Servicio Nacional de Geología y Minería, Santiago, pp. 246, 7 mapas escala 1:100.000.
- Sepúlveda, F.A. et al., 2012. Mapa geológico de Oficina Victoria, Región de Tarapacá. In: Blanco, N., et al. (Eds.), *Levantamiento Geológico Para El Fomento de La Exploración de Recursos Minerales e Hídricos de La Cordillera de La Costa, Depresión Central y Precordillera de La Región de Tarapacá (20°S-21°S)*, Informe Registrado IR-12-50. Servicio Nacional de Geología y Minería, Santiago, pp. 246, 7 mapas escala 1:100.000.
- Skarmeta, J., Marinovic, N., 1981. Hoja Quillagua, escala 1:250.000: Carta Geológica de Chile No. 51. Instituto de Investigaciones Geológicas.
- Starke, J. et al., 2017. Tectonic and climatic controls on the spatial distribution of denudation rates in northern Chile (18° S to 23° S) determined from cosmogenic nuclides. *J. Geophys. Res. Earth Surf.* 122, 1949–1971.
- Stuut, J.-B.W., Lamy, F., 2004. Climate variability at the southern boundaries of the Namib (southwestern Africa) and Atacama (northern Chile) coastal deserts during the last 120,000 yr. *Quat. Res.* 62, 301–309.
- Thomsen, K.J. et al., 2008. Laboratory fading rates of various luminescence signals from feldspar-rich sediment extracts. *Radiat. Meas.* 43, 1474–1486.
- Vargas, G. et al., 2006. ENSO tropical-extratropical climate teleconnections and mechanisms for Holocene debris flows along the hyperarid coast of western South America (17°–24°S). *Earth Plant. Sci. Lett.* 249, 467–483.
- Vásquez, P., Sepúlveda F.A., 2012a. Mapa geológico de Patillos, Región de Tarapacá. In: Blanco, N., et al. (Eds.), *Levantamiento Geológico Para El Fomento de La Exploración de Recursos Minerales e Hídricos de La Cordillera de La Costa, Depresión Central y Precordillera de La Región de Tarapacá (20°S-21°S)*, Informe Registrado IR-12-50. Servicio Nacional de Geología y Minería, Santiago, pp. 246, 7 mapas escala 1:100.000.
- Vásquez, P., Sepúlveda F.A., 2012b. Mapa geológico de Pozo Almonte, Región de Tarapacá. In: Blanco, N., et al. (Eds.), *Levantamiento Geológico Para El Fomento de La Exploración de Recursos Minerales e Hídricos de La Cordillera de La Costa, Depresión Central y Precordillera de La Región de Tarapacá (20°S-21°S)*, Informe Registrado IR-12-50. Servicio Nacional de Geología y Minería, Santiago, pp. 246, 7 mapas escala 1:100.000.
- Vásquez, P. et al., 2018. Cartas Guanillos del Norte y Salar de Llamara, Regiones de Tarapacá y Antofagasta, Serie Geología Básica 195-196. Servicio Nacional de Geología y Minería, Santiago, pp. 100, 1 mapa escala 1:100.000.
- Walk, J., submitted. Alluvial fans along the coastal Atacama Desert – landforms, processes, and evolution. Dissertation. RWTH Aachen University.
- Walk, J. et al., 2020. Gradients in climate, geology, and topography affecting coastal alluvial fan morphodynamics in hyperarid regions – the Atacama perspective. *Global Planet. Change* 185, 102994.